Sensors and Actuators A 219 (2014) 94–99

Contents lists available at ScienceDirect

Sensors and Actuators A: Physical

journal homepage: www.elsevier.com/locate/sna

Refractive index and strain sensing using inline Mach–Zehnder interferometer comprising perfluorinated graded-index plastic optical fiber

A.A. Jasim[a,b], N. Hayashi[c], S.W. Harun[a,b,*], H. Ahmad[b], R. Penny[b], Y. Mizuno[c], K. Nakamura[c]

[a] Department of Electrical Engineering, Faculty of Engineering, University of Malaya, Kuala Lumpur 50603, Malaysia
[b] Photonics Research Center, University of Malaya, Kuala Lumpur 50603, Malaysia
[c] Precision and Intelligence Laboratory, Tokyo Institute of Technology, Yokohama 226-8503, Japan

ARTICLE INFO

Article history:
Received 18 April 2014
Received in revised form 23 July 2014
Accepted 23 July 2014
Available online 19 August 2014

Keywords:
Tapered fibers
Plastic optical fibers
Heat-and-pull technique
Inline Mach–Zehnder interferometry
Refractive-index sensing
Strain sensing

ABSTRACT

This paper details the fabrication and performance evaluation of an inline Mach–Zehnder interferometer (MZI) consisting of a perfluorinated graded-index plastic optical fiber fabricated via a heat-and-pull tapering technique. This MZI exhibits interference fringes that are sufficiently sharp for usage as refractive-index (RI) and strain sensors. These interference fringes shift linearly with the RI of the surrounding medium, with a proportionality constant of 3.44 nm/RI unit. The measured strain sensitivity of 0.2 pm/$\mu\varepsilon$ suggests that the MZI may be viable for strain-sensing applications.

© 2014 Elsevier B.V. All rights reserved.

1. Introduction

Fiber inline interferometric sensors (FIISs) have drawn great interest in recent years thanks to their compactness, high sensitivity, ease of fabrication, and feasibility with a variety of measurands such as temperature, strain, and refractive index (RI). Several FIIS configurations have already been developed, including Mach–Zehnder interferometers (MZIs) based on photonic crystal fibers (PCFs) [1,2] or long-period fiber gratings (LPFGs) [3], and Fabry–Perot interferometers based on micro-holes [4] or hollow-core PCFs [5,6]. Such FIISs have the disadvantage of requiring high-cost specialty fibers and/or large dimensions. Consequently, FIISs utilizing tapered optical fibers, with the associated benefits of cost efficiency and smaller size [7], have attracted considerable interest. Taper-based FIISs, until now, have been exclusively fabricated using glass optical fibers that are too fragile to withstand strains beyond roughly 3%. Replacing the glass optical fibers with plastic (or polymer) optical fibers (POFs) [8–14] is a promising approach to overcome this limitation, offering advantages including ease of handling, high mechanical strength and load resistance, extremely high flexibility, and tolerance of strains in excess of 50%. Although some sensing applications of tapered POFs have already been demonstrated [15–19], no reports on the fabrication and characterization of POF-based inline interferometric RI/strain sensors have been published to the best of the authors' knowledge.

This paper reports on the first tests of an inline MZI made from a perfluorinated graded-index (GI-) POF, tapered by a heat-and-pull technique, along with an evaluation of its potential application as an RI and strain sensor. While the concept of using an MZI for measuring phase shift in the POF as a function of nominal strain has been reported previously [20], the assembly required a complex setup involving several components for configuring the MZI. In contrast, the experiment described in this paper uses a very short length of (GI-) POF, measuring approximately 10 mm, to fabricate an inline MZI of simple design that is suitable for use as an RI and strain sensor. Experimental results show that the interference fringes shift in proportion to the RI of a surrounding medium with a proportionality constant of 3.44 nm/RI unit and a linear correlation of 98%. In addition, the MZI sensitivity was measured at 0.2 pm/$\mu\varepsilon$, indicating that the device may be regarded as a strain sensor.

* Corresponding author at: Department of Electrical Engineering, Faculty of Engineering, University of Malaya, Kuala Lumpur 50603, Malaysia. Tel.: +60 379674290.
E-mail address: swharun@gmail.com (S.W. Harun).

http://dx.doi.org/10.1016/j.sna.2014.07.018
0924-4247/© 2014 Elsevier B.V. All rights reserved.

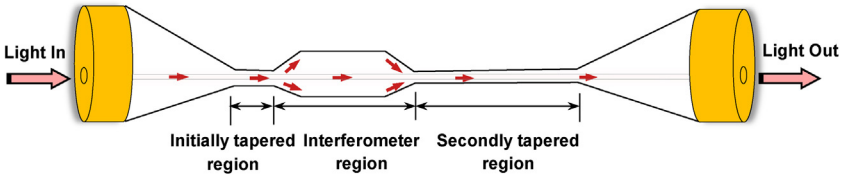

Fig. 1. Schematic diagram of the inline MZI.

2. Principles of inline MZIs

A diagram illustrating the principles of the inline MZI operation is shown in Fig. 1, and the intensity transfer function can be expressed generally by a two-beam optical interference equation:

$$I = I_1 + I_2 + 2\sqrt{I_1 I_2}\cos(\varphi), \tag{1}$$

where I is the intensity of the interference signal, and I_1 and I_2 are the intensities of the light propagating in the fiber core and cladding, respectively. The phase difference between the core and cladding modes is φ, which is approximately equal to

$$\varphi = \left(\frac{2\pi(\Delta n_{\text{eff}})L_{\text{eff}}}{\lambda}\right), \tag{2}$$

where Δn_{eff} is defined as $(\Delta n_c^{\text{eff}} - n_{cl,m}^{\text{eff}})$, i.e. the difference between the effective RIs of the core mode and the m-th order cladding mode respectively, L_{eff} is the effective length of the interferometer, and λ is the optical wavelength. Eq. (2) indicates that the phase difference between the core and cladding modes is directly dependent on the difference in their effective RI as well as the effective length of the interferometer. Input light in an inline MZI is generally split into guided and unguided modes at the interference region; guided modes continue to travel in the core, while unguided modes extend through the cladding–air interface, thus allowing the evanescent field to react with the ambient medium. An interference signal occurs when the two modes are recombined in the second tapered region. This reaches a minimum intensity ($I = I_{\min}$) when the phase difference between the core and cladding modes satisfies the condition $\varphi = (2k+1)\pi$, where k is an integer. The attenuation peak wavelength λ_v of the kth order can then be expressed as

$$\lambda_v = \frac{2(n_c^{\text{eff}} - n_{cl,m}^{\text{eff}})L_{\text{eff}}}{(2k+1)}. \tag{3}$$

In general, the cladding modes at the tapered sections are readily affected by the RI of the surrounding medium, and thus the effective RI of the cladding modes $n_{cl,m}^{\text{eff}}$ is highly sensitive to RI variations in the surrounding medium. The effective RI of the core modes n_c^{eff} does not vary with the ambient index change, and is thus highly invariant. Therefore, the relationship of $n_{cl,m}^{\text{eff}}$ with respect to λ_v is given as

$$\frac{d\lambda_v}{dn_{cl,m}^{\text{eff}}} = \frac{2\pi L_{\text{eff}}}{(2k+1)\pi} = \frac{\lambda_v}{(n_{cl,m}^{\text{eff}} - n_c^{\text{eff}})}, \tag{4}$$

Consequently, it can be asserted that the RI-sensing mechanism of the inline MZI relies on the shifting of the attenuation peak wavelength λ_v from the variation of ambient RI, whereby a change occurs in effective RI difference Δn_{eff} between the core and cladding modes. The strain-sensing mechanism of the inline MZI relies on the shift in λ_v from the elongation of the interferometer, causing a change both in L_{eff} and Δn_{eff}.

3. Fabrication and characterization of inline MZIs

Two typical commercially available POFs are poly(methyl methacrylate)-based POFs [8,9] and perfluorinated GI-POFs [10–14]. The former transmit mainly visible light at around 650 nm, whereas the latter transmit both visible light and telecom-wavelength light. An amplified spontaneous emission (ASE) source at 1.55 μm was used in this experiment, and so the inline MZI was fabricated from a perfluorinated GI-POF. The core and cladding layers of the GI-POF consisted of doped and undoped amorphous perfluorinated polymer (polyperfluorobutenylvinyl ether), respectively. The RI at the center of the core was 1.356, whereas that of the cladding layer was 1.342. The numerical aperture (NA) was 0.185 and the core/cladding diameters were 50/100 μm. This GI-POF has a 750 μm diameter polycarbonate reinforcement over-cladding layer, which reduces microbending loss and increases load-bearing capability. Propagation loss at 1.55 μm wavelength was approximately 250 dB/km.

Fig. 2 shows a schematic for fabricating a POF-based inline MZI, where a meter-long POF was affixed using two linear translation stages. A solder gun set at 110 °C was placed 5 cm below the POF, acting as a heat source. Both ends of the POF were butt-coupled [12] to standard silica single-mode fibers (SMFs), i.e., the ends of

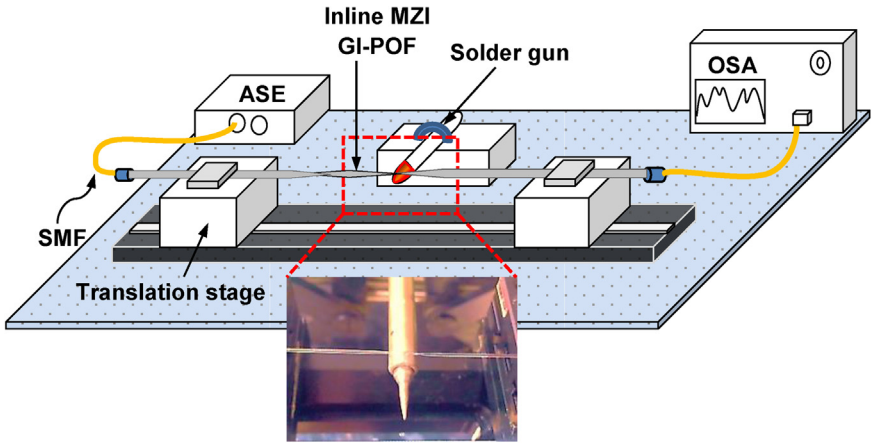

Fig. 2. Schematic for fabricating an inline MZI.

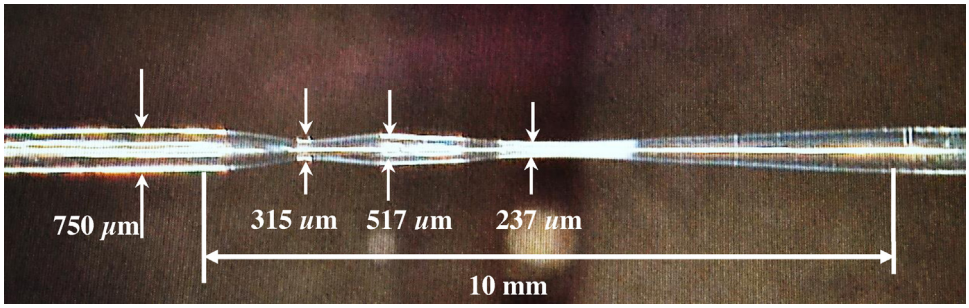

Fig. 3. An optical microscope image of the fabricated inline MZI.

the SMFs fitted with 'FC' connectors were attached to both ends of the POF fitted with 'SC' connectors via 'FC/SC' adaptors. This configuration resulted in precisely aligned cores predominantly exciting the fundamental propagation mode. One SMF was connected to a broadband ASE source and the other SMF was connected to an optical spectrum analyzer (OSA). A portion of the POF was heated to a softening temperature then stretched until the over-cladding diameter was reduced to 315 μm. The solder gun was then moved to one side of the POF, allowing another POF section to be tapered further until the over-cladding diameter decreased to 237 μm. An optical microscope image of the POF-based inline MZI fabricated by this process is shown in Fig. 3, where the total tapered length is approximately 10 mm. Fig. 4 shows the output spectrum of the inline MZI alongside the incident ASE spectrum. The dashed line in Fig. 4 represents the transmission spectrum normalized to the input ASE spectrum, which contributes to an improved visibility. The ~35-dB insertion loss of the inline MZI results predominantly from inefficient coupling at the interfaces between the silica SMF and the POF.

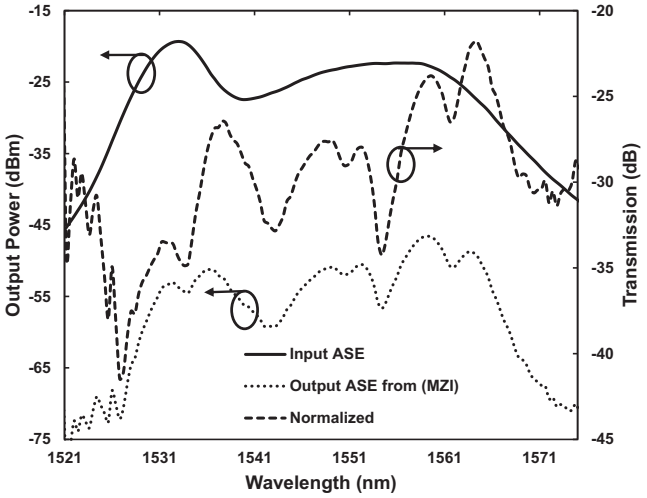

Fig. 4. Spectra from the incident ASE, and the inline MZI output.

4. Applications of inline MZI for RI and strain sensing

Fig. 5 shows the RI-sensing experimental setup, where the POF-based inline MZI is placed in a plastic container filled with air, water, or one of four types of oil. These oils are differentiated by their respective RIs, ranging from 1.44 to 1.74. The OSA is used to measure the change in output spectrum, which is a function of RI. Fig. 6(a) shows the transmitted interference spectra at around 1537 nm for the six fluids, where the wavelengths of the spectral peaks are red-shifted with increasing RI from 1.00 to 1.74. Noticeable red-shifting occurs under these conditions because the higher-order cladding mode makes a significant contribution to the light interference, which is a result of the non-uniform tapering shape of the inline MZI. Moreover, according to Eq. (4), the shifting of $d\lambda_v/dn_{cl,m}^{\text{eff}}$ varies for different mth order cladding modes. A similar phenomenon was observed for the standard silica SMFs and LPFG-based RI sensors [21,22]. It can be also observed from Fig. 6(a) that the peak power of the wavelength decreases with increasing RI. An increase in RI causing this reduction of power can

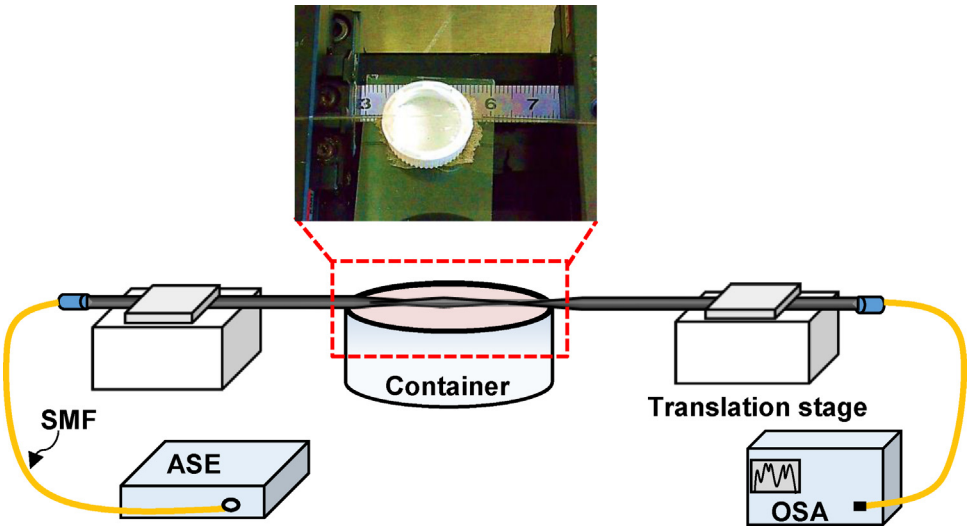

Fig. 5. Schematic for RI sensing.

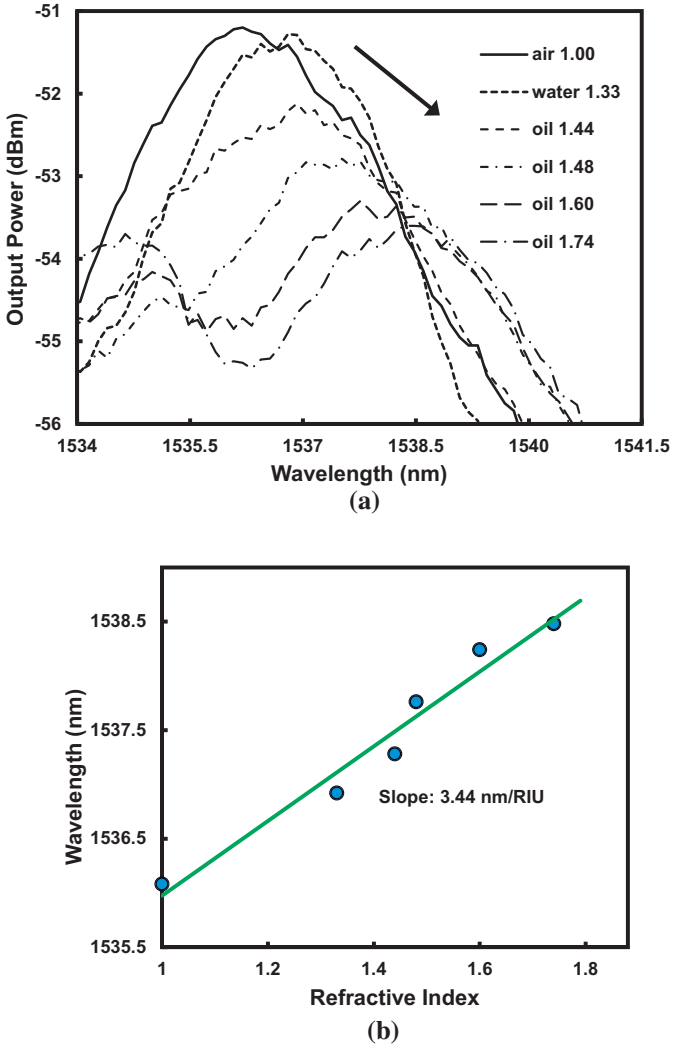

Fig. 6. (a) Transmitted interference spectra at around 1537 nm with six fluids used. (b) Peak wavelength correlation with RI.

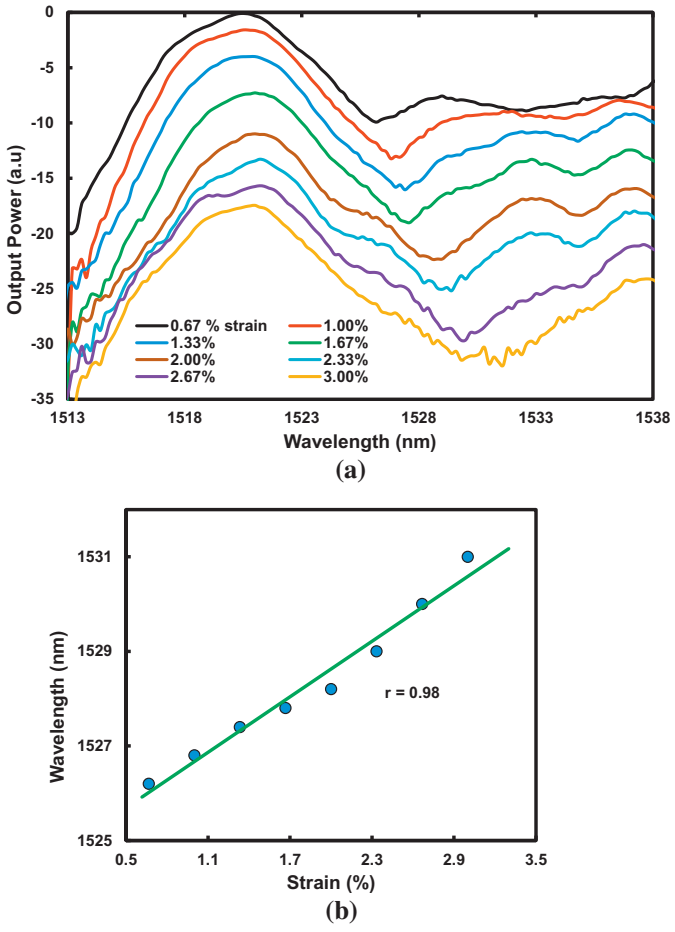

Fig. 7. (a) Transmitted interference spectra at around 1528 nm with different strains applied. (b) Dip wavelength correlation with strain.

be attributed to most of the cladding modes' power being absorbed in the surrounding high-RI medium. The peak wavelength is plotted as a function of RI as shown in Fig. 6(b). This dependence shows a strong linear fit, with a correlation coefficient of $r > 0.98$ and a sensitivity of 3.44 nm/RI unit (RIU). This value is much lower than the sensitivities of standard silica SMF-, PCF-, and LPG-based RI sensors, which are on the order of hundreds of nm/RIU [22–24]. This reduced sensitivity occurs mainly because the diameter of the fabricated POF-based inline MZI is much greater than the diameters of the other fibers. Enhancing the RI sensitivity will require a thinner POF adopted in the fabrication of the inline MZI, as well as an increase in interferometer length. Such measures should increase the cladding modes' propagation into the ambient medium, and thus lead to $n_{cl,m}^{\text{eff}}$ being affected significantly with the change of the ambient RI. In practice, this inline MZI sensor is capable of monitoring an aqueous medium with refractive index ranging from 1.33 to 1.74.

The strain dependence of the transmitted interference spectra near 1528 nm at room temperature was also investigated. One end of the inline MZI was fixed on a stationary platform and the other end was set on a translation stage with a calibrated 1-μm screw clamp having a resolution of 2 μm/step. The gauge length between two stages was 60 mm, and the POF-based inline MZI was held taut across this region. Strains of up to 3%, corresponding to 1.8 mm of the gauge length, were applied to the POF-based inline MZI. Fig. 7(a) shows the resulting spectral variation for applied strains of 0.67–3.00%, where the spectral dip experiences an increased redshift with additional strain. This correlation arises because, in this setup, the interferometer elongation has a greater impact on wavelength than changes in Δn_{eff}, resulting in a phase shift toward longer wavelength. Strain dependence on the wavelength at the spectral dip also shows a strong linear fit with a correlation of $r > 0.98$ and a sensitivity of 0.2 pm/με, as shown in Fig. 7(b).

The inline MZI strain sensitivity is lower than the 1.2 pm/με result from strain applied to fiber Bragg gratings fabricated in uniform-waist fiber tapers [25]. This relative drop in sensitivity can be explained by taking into account the non-uniform, tapered shape of the POF-based inline MZI; the two tapered regions experience an unequal strain due to local mechanical resistance, and this imbalance results in a reduction of sensitivity. Nevertheless, the strain sensitivity of the POF-based inline MZI remains comparable with that of the non-tapered LPFG all-solid photonic bandgap fiber, where the sensitivity difference observed is 0.792 pm/με [26]. Still, the fabricated inline MZI retains the relative advantages of design simplicity and lower cost. Moreover, POF-based sensors retain the key advantage of high flexibility, showing a much greater potential for large-strain sensing than that of glass-fiber-based sensors. Their thermal stability was also sufficiently high for practical applications. Issues with relatively low sensitivity and large loss could be mitigated: POFs with different structures such as smaller core diameters might improve the sensitivity, and propagation loss could be lowered to ~10 dB/km by using a

shorter source wavelength (1000–1100 nm or 1230 nm) [11]. Thus, overall, the POF-based inline MZI is suitable for applications as an RI and strain sensor.

5. Conclusion

Combined RI and strain sensing is demonstrated for the first time with an inline MZI made from a perfluorinated GI-POF tapered by a heat-and-pull technique. Interference fringes of the MZI are observed to shift toward longer wavelength when the RI of the surrounding medium increases from 1.00 to 1.74. The RI sensitivity is 3.44 nm/RIU. Strain-sensing capability with a sensitivity of 0.2 pm/$\mu\varepsilon$ was also confirmed. The authors believe these results will serve as an important guideline toward the development of more refined RI and strain sensors derived from POF-based inline MZIs.

Acknowledgement

The authors acknowledge the financial support from the University of Malaya and the Ministry of Higher Education (MOHE) under grants, UM.C/625/1/HIR/MOHE/SCI/29, RU002/2013 and PG139-2012B. This work was also partially supported by Grants-in-Aid for Young Scientists (A) (no. 25709032) and for Challenging Exploratory Research (no. 26630180) from the Japan Society for the Promotion of Science (JSPS), and research grants from the General Sekiyu Foundation, the Iwatani Naoji Foundation, and the SCAT Foundation. N.H. acknowledges a Grant-in-Aid for JSPS Fellows (No. 25007652).

References

[1] B. Kim, T.H. Kim, L. Cui, Y. Chung, Twin core photonic crystal fiber for in-line Mach–Zehnder interferometric sensing applications, Opt. Express 17 (2009) 15502–15507.
[2] W.J. Bock, T.A. Eftimov, P. Mikulic, J. Chen, An inline core-cladding intermodal interferometer using a photonic crystal fiber, J. Lightw. Technol. 27 (2009) 3933–3939.
[3] J.-F. Ding, A.P. Zhang, L.-Y. Shao, J.-H. Yan, S. He, Fiber-taper seeded long-period grating pair as a highly sensitive refractive-index sensor, Photonics Technol. Lett. IEEE 17 (2005) 1247–1249.
[4] C.R. Liao, T.Y. Hu, D.N. Wang, Optical fiber Fabry–Perot interferometer cavity fabricated by femtosecond laser micromachining and fusion splicing for refractive index sensing, Opt. Express 20 (2012) 22813–22818.
[5] M.S. Ferreira, J. Bierlich, J. Kobelke, K. Schuster, J.L. Santos, O. Frazão, Towards the control of highly sensitive Fabry–Pérot strain sensor based on hollow-core ring photonic crystal fiber, Opt. Express 20 (2012) 21946–21952.
[6] J. Villatoro, V. Finazzi, G. Coviello, V. Pruneri, Photonic-crystal-fiber-enabled micro-Fabry–Perot interferometer, Opt. Lett. 34 (2009) 2441–2443.
[7] Z. Tian, S. Yam, H. Loock, Refractive index sensor based on an abrupt taper Michelson interferometer in a single-mode fiber, Opt. Lett. 33 (2008) 1105–1107.
[8] M.G. Kuzyk, Polymer Fiber Optics: Materials, Physics, and Applications, CRC, Boca Raton, FL, USA, 2006.
[9] Y. Koike, T. Isigure, E. Nihei, High-bandwidth graded-index polymer optical fiber, J. Lightw. Technol. 13 (1995) 1475–1489.
[10] T. Ishigure, Y. Koike, J.W. Fleming, Optimum index profile of the perfluorinated polymer-based GI polymer optical fiber and its dispersion properties, J. Lightw. Technol. 18 (2000) 178–184.
[11] Y. Koike, M. Asai, The future of plastic optical fiber, NPG Asia Mater. 1 (2009) 22–28.
[12] Y. Mizuno, K. Nakamura, Experimental study of Brillouin scattering in perfluorinated polymer optical fiber at telecommunication wavelength, Appl. Phys. Lett. 97 (2010) 021103.
[13] N. Hayashi, Y. Mizuno, K. Nakamura, Brillouin gain spectrum dependence on large strain in perfluorinated graded-index polymer optical fiber, Opt. Express 20 (2012) 21101–21106.
[14] Y. Mizuno, N. Hayashi, H. Tanaka, K. Nakamura, S. Todoroki, Observation of polymer optical fiber fuse, Appl. Phys. Lett. 104 (2014) 043302.
[15] C. Pulido, Ó. Esteban, Improved fluorescence signal with tapered polymer optical fibers under side-illumination, Sens. Actuators: B. Chem. 146 (2010) 190–194.
[16] Y. Jeong, S. Bae, K. Oh, All fiber N × N fused tapered plastic optical fiber (POF) power splitters for photodynamic therapy applications, Curr. Appl. Phys. 9 (2009) e273–e275.
[17] A. Leung, P. Shankar, R. Mutharasan, Label-free detection of DNA hybridization using gold-coated tapered fiber optic biosensors (TFOBS) in a flow cell at 1310 nm and 1550 nm, Sens. Actuators B: Chem. 131 (2008) 640–645.
[18] C. Beres, F.V.B. de Nazaré, N.C.C. de Souza, M.A.L. Miguel, M.M. Werneck, Tapered plastic optical fiber-based biosensor – tests and application, Biosens. Bioelectron. 30 (2011) 328–332.
[19] J. Arrue, F. Jiménez, G. Aldabaldetreku, G. Durana, J. Zubia, M. Lomer, J. Mateo, Analysis of the use of tapered graded-index polymer optical fibers for refractive-index sensors, Opt. Express 16 (2008) 16616–16631.
[20] S. Kiesel, K. Peters, T. Hassan, M. Kowalsky, Calibration of a single-mode polymer optical fiber large-strain sensor, Meas. Sci. Technol. 20 (2009) 034016.
[21] P. Lu, L. Men, K. Sooley, Q. Chen, Tapered fiber Mach–Zehnder interferometer for simultaneous measurement of refractive index and temperature, Appl. Phys. Lett. 94 (2009) 131110.
[22] R. Yang, Y.-S. Yu, Y. Xue, C. Chen, Q.-D. Chen, H.-B. Sun, Single S-tapered fiber Mach–Zehnder interferometers, Opt. Lett. 36 (2011) 4482–4484.
[23] C. Li, S.-J. Qiu, Y. Chen, F. Xu, Y.-Q. Lu, Ultra-sensitive refractive index sensor with slightly tapered photonic crystal fiber, Photonics Technol. Lett. IEEE 24 (2012) 1771–1774.
[24] W.B. Ji, S.C. Tjin, B. Lin, C.L. Ng, Highly sensitive refractive index sensor based on adiabatically tapered microfiber long period gratings, Sensors 13 (2013) 14055–14063.
[25] T. Wieduwilt, S. Brückner, H. Bartelt, High force measurement sensitivity with fiber Bragg gratings fabricated in uniform-waist fiber tapers, Meas. Sci. Technol. 22 (2011) 075201.
[26] Q. Huang, Y. Yu, Z. Ou, X. Chen, J. Wang, P. Yan, C. Du, Refractive index and strain sensitivities of a long period fiber grating, Photonic Sens. 4 (2014) 92–96.

Biographies

A.A. Jasim received a B.Sc. degree in Electrical Engineering from the University of Technology, Baghdad, Iraq, in 2007, and M.E. and Ph.D. degrees in Photonic and Fiber Optic Technology from the University of Malaya, Malaysia, in 2010 and 2014, respectively. He is currently a Research Fellow at the Photonics Research Centre, University of Malaya. His research interest is in optical micro/nanofiber photonic devices and their applications.

N. Hayashi received his received a B.E. degree in Advanced Production from the Gunma National College Technology, Japan, in 2011, and an M.E. degree in Electronic Engineering from the Tokyo Institute of Technology, Japan, in 2013. He is currently studying polymer optics for his Dr. Eng. degree at the Tokyo Institute of Technology.

S.W. Harun received a B.E. degree in Electrical and Electronics System Engineering from the Nagaoka University of Technology, Japan in 1996, and M.Sc. and Ph.D. degrees in Photonics from the University of Malaya in 2001 and 2004, respectively. Currently, he is a full professor at the Faculty of Engineering, University of Malaya. His research interests include fiber-optic active and passive devices.

H. Ahmad received a Ph.D. degree in laser technology from the University of Swansea (UK) in 1983. He is a full professor at the Department of Physics and director of the Photonics Research Centre, University of Malaya. He is also a fellow member of the Malaysian Academic of Science.

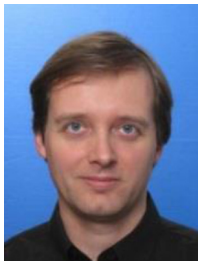

R. Penny received a Ph.D degree in high energy physics from the University of Birmingham (UK) in 2004. He is currently a research consultant at the Photonics Research Centre, University of Malaya.

Y. Mizuno received B.E., M.E., and Dr. Eng. degrees in Electronic Engineering from the University of Tokyo, Japan, in 2005, 2007, and 2010, respectively. He is currently an Assistant Professor at Precision and Intelligence Laboratory, Tokyo Institute of Technology, where he is active in fiber-optic sensing, polymer optics, and ultrasonics.

K. Nakamura received B.E., M.E., and Dr. Eng. degrees from Tokyo Institute of Technology, Japan, in 1987, 1989, and 1992, respectively. He is currently a Professor at the Precision and Intelligence Laboratory, Tokyo Institute of Technology. His field of research is the applications of ultrasonic waves, measurement of vibration and sound using optical methods, and fiber-optic sensing.